

Spatiotemporal dynamics of γ H2AX in the mouse brain after acute irradiation at different postnatal days with special reference to the dentate gyrus of the hippocampus

Feng Ru Tang¹, Lian Liu², Hong Wang¹, Kimberly Jen Ni Ho¹, Gautam Sethi³

¹Radiation Physiology Lab, Singapore Nuclear Research and Safety Initiative, National University of Singapore, Singapore 138602, Singapore

²The School of Basic Medicine, Health Science Center, Yangtze University, Jingzhou 434023, Hubei, China

³Department of Pharmacology, Yong Loo Lin School of Medicine, National University of Singapore, Singapore 117600, Singapore

Correspondence to: Feng Ru Tang, Gautam Sethi; **email:** tangfr@gmail.com, <https://orcid.org/0000-0003-2462-1787>; phcgs@nus.edu.sg

Keywords: γ H2AX, radiation, spatiotemporal dynamics, brain, dentate gyrus

Received: February 17, 2021

Accepted: June 4, 2021

Published: June 23, 2021

Copyright: © 2021 Tang et al. This is an open access article distributed under the terms of the [Creative Commons Attribution License](https://creativecommons.org/licenses/by/3.0/) (CC BY 3.0), which permits unrestricted use, distribution, and reproduction in any medium, provided the original author and source are credited.

ABSTRACT

Gamma H2A histone family member X (γ H2AX) is a molecular marker of aging and disease. However, radiosensitivity of the different brain cells, including neurons, glial cells, cells in cerebrovascular system, epithelial cells in pia mater, ependymal cells lining the ventricles of the brain in immature animals at different postnatal days remains unknown. Whether radiation-induced γ H2AX foci in immature brain persist in adult animals still needs to be investigated. Hence, using a mouse model, we showed an extensive postnatal age-dependent induction of γ H2AX foci in different brain regions at 1 day after whole body gamma irradiation with 5Gy at postnatal day 3 (P3), P10 and P21. P3 mouse brain epithelial cells in pia mater, glial cells in white matter and cells in cerebrovascular system were more radiosensitive at one day after radiation exposure than those from P10 and P21 mice. Persistent DNA damage foci (PDDF) were consistently demonstrated in the brain at 120 days and 15 months after irradiation at P3, P10 and P21, and these mice had shortened lifespan compared to the age-matched control. Our results suggest that early life irradiation-induced PDDF at later stages of animal life may be related to the brain aging and shortened life expectancy of irradiated animals.

INTRODUCTION

Gamma H2A histone family member X (γ H2AX) is a phosphorylated H2AX on serine 139. While the number of its initial foci increases in lymphocytes immediately after radiation exposure, it is reduced with deoxyribonucleic acid (DNA) double-strand break (DSB) repair after acute radiation exposure. However, some fractions of foci may persist depending on radiation doses and cell types. γ H2AX foci have therefore been considered as a sensitive biomarker for DSB and repair at the early stage [1, 2], and for ageing and gene

silencing in unreparable DNA damaged neurons at the late stages of radiation exposure [3–6]. γ H2AX may also be involved in the brain damage and can also play a part in different neurological and neuropsychological disorders. For instance, it has been reported to be involved in the excitotoxicity induced by glutamate receptor activation and seizures [7, 8], in the pathogenesis of Alzheimer's disease (AD) [9], Huntington's disease [10], and depression-related cellular senescence [11]. γ H2AX has also been reported to be related to the fate of neuronal precursors at different pre- and post-natal stages of animal life

including aged mice [5], as well as being involved in the regulation of necrosis in glioblastoma after irradiation [12]. A number of previous studies have suggested that radiation exposure may induce depression [13–16], AD [15, 17], and schizophrenia [15, 18]. Thus, understanding the spatiotemporal dynamics of brain γ H2AX after irradiation at an early life of animal may be important for monitoring life-time radiation effect on neurodegeneration and brain aging. It can also be used for evaluating the therapeutic effects of radio-neuro-protective drugs and for designing novel therapy by targeting γ H2AX protein to promote neural repair process, as well to prevent the development of neurological and neuropsychological disorders.

This study aimed to investigate the spatiotemporal dynamics of γ H2AX expression in the mouse brain, in particular, dentate gyrus after acute radiation exposure. The findings may reveal 1) if there existed a significant difference in brain radiosensitivity among mice irradiated at postnatal day 3 (P3), P10 and P21; 2) where or which types of brain cells, i.e., neurons, different glial cells, epithelial cells in pia mater, cells in the blood vessel were γ H2AX foci localized; 3) if irradiation induced persistent DNA damage foci (PDDF) in the brain cells at the chronic stages after radiation exposure.

RESULTS

Acute irradiation-induced brain γ H2AX changes

Irradiation at P3

In the control P4 (P3+1C, i.e., 1 day after pseudo radiation exposure on P3), P10 (P3+7C, i.e., 7 days after pseudo radiation exposure on P3), P120-C (i.e., 120 days after pseudo radiation exposure on P3) mice without radiation exposure, very few γ H2AX foci could be observed in different brain regions (Figures 1A–1D, 2A–2D, 3A, 3A', Figure 4A, Figure 5) (Table 1). However, acute irradiation with 5Gy at P3 induced significant γ H2AX expression in the entire brain 1 day after radiation exposure. γ H2AX foci could be observed in almost all parts of brain region. It included dorsal pallium (DPall) /isocortex (from the outer pia mater, all layers of the grey matter, white matter to the subventricular zone), medial pallium (MPall) (hippocampal allocortex including the hilus, strata granulosum and moleculare of the dentate gyrus, strata laculosum moleculare, radiatum, pyramidale, oriens of CA1-3 areas), central subpallium/classic basal ganglia (CSPall), alar plate of evaginated telencephalic vesicle (TelA); prosomere 1-3 (Figure 1A'–1D', 1A''–1D'', Figure 2A'–2D', 2A''–2D'', Figure 3B, 3C) (refer to “The Allen Developing Mouse Brain Atlas,

P4”, website: <https://atlas.brain-map.org/atlas?atlas=181276162#atlas=181276162&plate=100711203&structure=15818&x=3841&y=3440&zoom=-3&resolution=7.92&z=7>). γ H2AX foci were demonstrated in almost all types of brain cells including epithelial cells in pia mater (Figure 1A', 1A''), different cells (neurons and glial cells) in the cortex (Figures 1B', 1B'', 1C', 1C'', 2A'–2D'', 2A''–2D'), glial cells in the white matter (Figure 1D', 1D'') and cells in the blood vessel (Figure 3B', 3C').

In the subventricular zone (SVZ), rostral migratory stream (RMS) and temporal migratory stream (TMS) (Figures 2A', 2C', 2A'', 2C'') and olfactory bulb (OB), the subgranular zone (SGZ) of the dentate gyrus (Figure 2B', 2B''), in the principal neurons in the strata pyramidale (Figure 3B, 3C) and granulosum and interneurons in other layers of the hippocampus, at the border between dorsal hippocampus and corpus callosum (Figure 2D', 2D''), many γ H2AX foci were also found. Hematoxylin-stained apoptotic bodies or pyknotic nuclei were observed in different brain regions, in particular, in those parts that are involved in neurogenesis and neuronal migration, i.e., SVZ, SGZ, OB, RMS and TMS (Figure 2A'–2D', Figure 2A''–2D'').

Seven days (P3+7) after irradiation with 5 Gy at P3, many γ H2AX foci still existed in the most of the brain regions. However, no γ H2AX foci appeared in the pia mater, white matter, the stratum moleculare of the dentate gyrus, strata laculosum moleculare, radiatum, oriens of CA1-3 areas of the hippocampus and cerebrovascular system (Table 1).

Irradiation at P10 or P21

One day after irradiation at P10 or P21, many γ H2AX foci were observed in the layers II to VI of the DPall, in the stratum pyramidale of CA1-3 areas and stratum granulosum of the dentate gyrus in MPall (Table 1). They were also found in the brain regions involved in neurogenesis and neuronal migration, i.e., SVZ, SGZ, olfactory bulb (OB), rostral migratory stream (RMS) and temporal migratory stream (TMS) (TelA) and CSPall. Increased γ H2AX foci were also demonstrated in the striatum and thalamus. However, there was no obvious change of γ H2AX foci in the pia mater, white matter, the stratum moleculare of the dentate gyrus, strata laculosum moleculare, radiatum, oriens of CA1-3 areas of the hippocampus in MPall and in the cerebrovascular system (Table 1). These changes were similar to those occurred at 7 days after irradiation at P3. At 7 days after irradiation at P10, there was similar patterns of γ H2AX foci distribution to 1 day after irradiation.

Four months (120 days) after irradiation with 5 Gy at P3, P10 and P21, some γ H2AX foci or PDDF could still

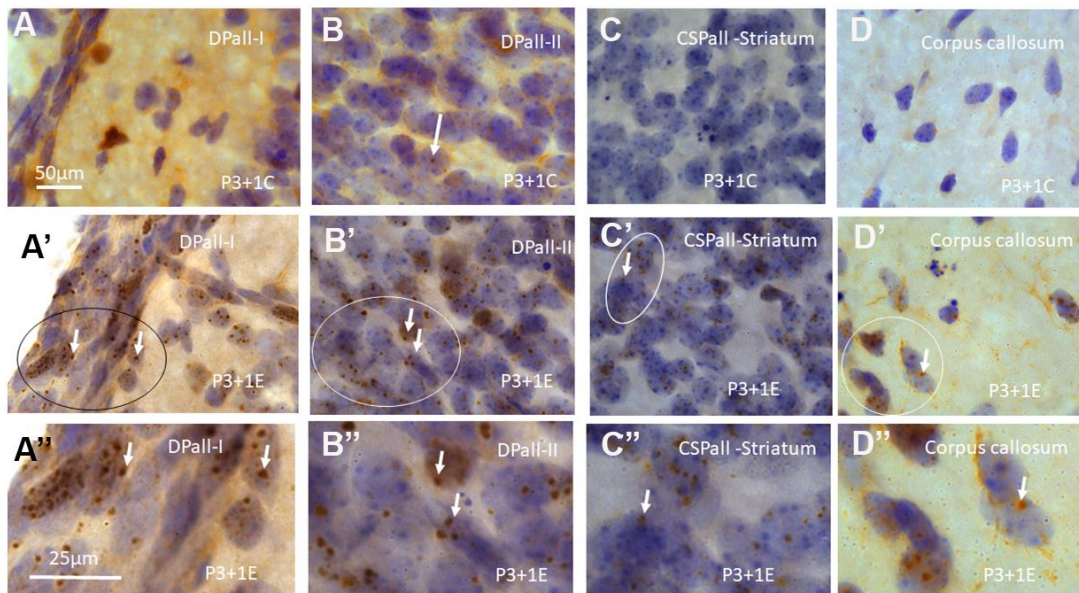


Figure 1. γ H2AX immunostaining counterstained with hematoxylin shows very few γ H2AX foci in different brain regions of postnatal day 4 (P4) mice without irradiation including dorsal pallium(DPall) /isocortex layer I (DPall-I) and pia mater (A), DPall-II (B, arrow), central subpallium/classic basal ganglia (CSPall) striatum (C) and corpus callosum (D). However, acute irradiation with 5Gy at P3 induced very significant γ H2AX expression in the entire brain 1 day after radiation exposure or P4 mice. γ H2AX foci could be observed in almost all brain regions at 1 day after irradiation at P3, including DPall-I (A', A' is magnified from the ellipse in A'), DPall-II to DPall-VI of the grey mater (B', B', DPall-II, B' is magnified from the ellipse in B'), CSPall striatum (C', C' is magnified from the ellipse in C') and corpus callosum (D', D' is magnified from the ellipse in D') at 1 day after irradiation at P3. Scan bar=50 μ m in (A) applies to (B-D) (A'-D') Scan bar=25 μ m in (A'') applies to (B''-D'').

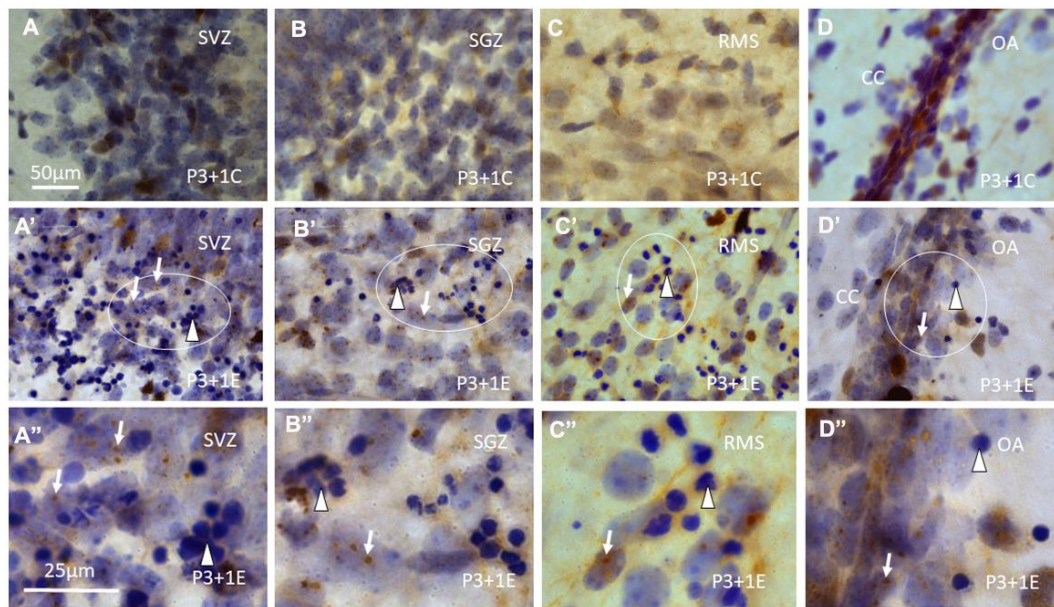


Figure 2. γ H2AX immunostaining counterstained with hematoxylin shows that γ H2AX foci are almost undetectable in the subventricular zone (SVZ) (A) of the lateral ventricle, subgranular zone (SGZ) (B), rostral migratory stream (RMS) (C) and the border between dorsal hippocampus (O/A: border between stratum oriens and alveus) and corpus callosum (CC) (D) of P4 mice without irradiation. Irradiation with 5Gy induced obvious γ H2AX foci (arrows) in SVZ (A', A' is magnified from the ellipse in A'), SGZ (B', B' is magnified from the ellipse in B'), RMS (C', C' is magnified from the ellipse in C') and the border between O/A and CC (D', D' is magnified from the ellipse in D'). Furthermore, many apoptotic bodies (arrowheads) appear in SVZ (A', A''), SGZ (B', B''), RMS (C', C'') and the border between O/A and CC (D', D'') at 1 day after irradiation at P3. Scan bar=50 μ m in (A) applies to (B-D) (A'-D') Scan bar=25 μ m in (A'') applies to (B''-D'').

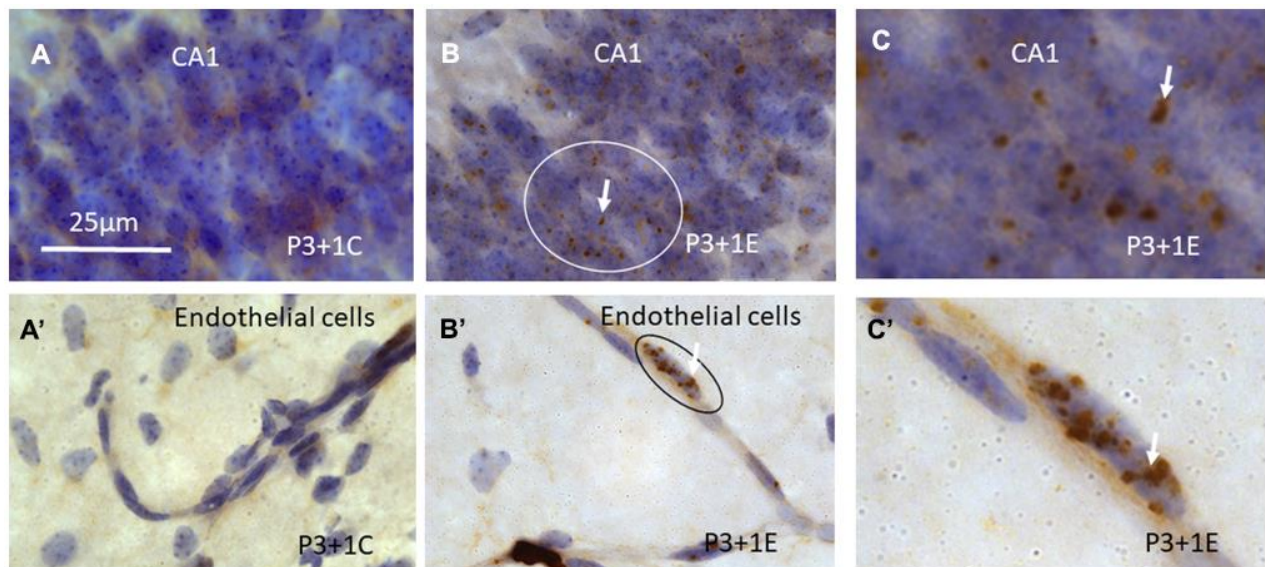


Figure 3. γ H2AX immunostaining counterstained with hematoxylin shows that γ H2AX foci are almost undetectable in the stratum pyramidale of CA1 area of the hippocampus (A) of P4 mice without irradiation. Irradiation with 5Gy induced obvious γ H2AX foci (arrows) in the stratum pyramidale of CA1 area (B, C is magnified from the ellipse in B) at 1 day after irradiation at P3. Similarly, γ H2AX foci are undetectable in the blood vessel of the hippocampus (A') of P4 mice without irradiation. Irradiation induced obvious γ H2AX foci (arrows) in the hippocampal blood vessel (B', C' is magnified from the ellipse in B') at 1 day after irradiation at P3. Scan bar=25 μ m in (A) applies to (B–C) (A'–C').

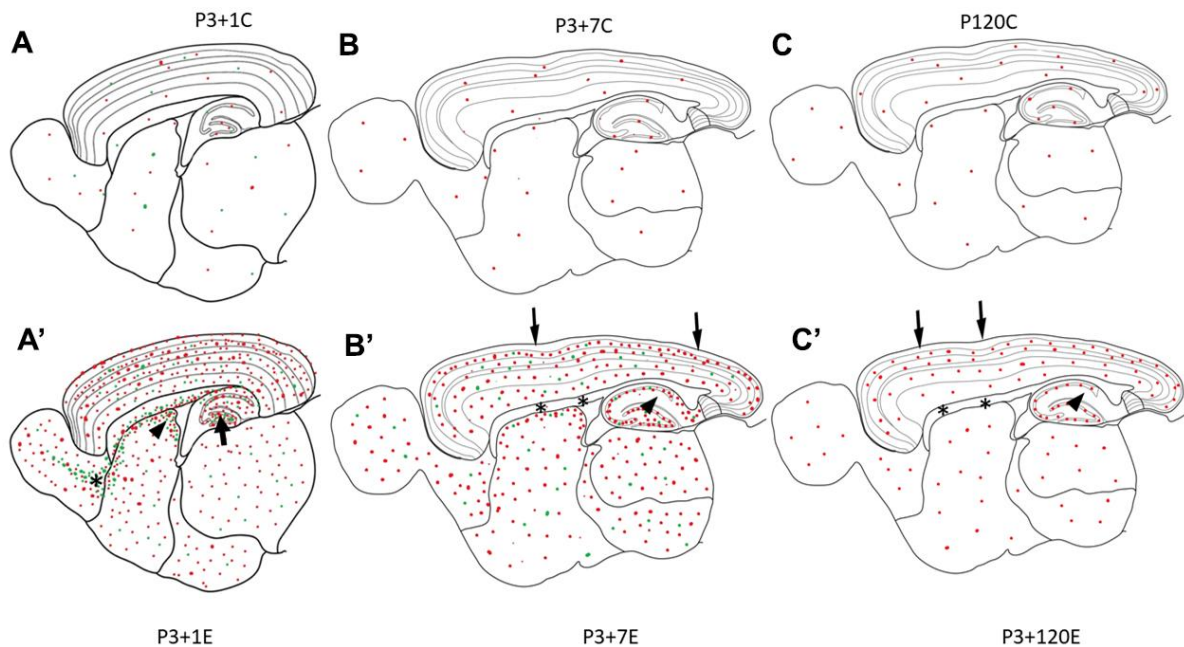


Figure 4. Diagrams (A–C) show γ H2AX foci (red dots) in the brain of the control animal without irradiation. In P3+1C or P4 mouse brain, a few apoptotic bodies (green dots) randomly appear in different brain regions (A). One day after irradiation at P3, γ H2AX foci (red dots) and apoptotic bodies (green dots) increase obviously in all brain regions (A'). Drastic increase of apoptotic bodies (green dots) appear in the hilus of the dentate gyrus (arrow), in the subventricular zone of the lateral ventricle (arrowhead) and in the rostral migratory stream (asterisk) (A'). Seven days after irradiation at P3, many γ H2AX foci (red dots) and apoptotic bodies (green dots) still exist in all brain regions (B'). However, there was no obvious change of γ H2AX foci in the pia mater (arrow), white matter (corpus callosum, asterisks), the strata lacunosum moleculare, radiatum (arrow), oriens of CA1-3 areas, the stratum moleculare of the dentate gyrus (B'). One hundred-twenty days after irradiation at P3, there are still some γ H2AX foci (red dots) still exist in all brain regions (C') although the number of γ H2AX foci is reduced obviously.

be observed in the layers II-III of cortex (Figure 6A), the stratum granulosum of the dentate gyrus (Figure 6B), and the stratum pyramidale of CA1-3 areas of the hippocampus (Figure 6C). γ H2AX foci were almost undetectable in the corpus callosum although these foci still existed in the striatum (Figure 6E), thalamus (Figure 6F), olfactory bulb (Figure 6G) and subventricular zone of the lateral ventricle (Figure 4, Figure 6H) (Table 1) although the number of γ H2AX foci was decreased when compared to those at 1 and 7 days after radiation exposure.

Fifteen months (15M) after irradiation at P3, P10 and P21, similar γ -H2AX foci or PDDF could be observed as those at 120 days in the layers II-III of cortex (Figure 7A). They were also noted in the stratum granulosum of the dentate gyrus (Figure 7B), and the stratum pyramidale of CA1-3 areas of the hippocampus (Figure 7C), in the striatum (Figure 7D), thalamus (Figure 7E), olfactory bulb (Figure 7F) (Table 1). It suggested that γ -H2AX foci might be localized in those neurons involved in major brain activities such as sensation, locomotor, and learning and memory.

γ H2AX foci in the stratum granulosum of the dentate gyrus

Quantitative study of γ H2AX foci in the stratum granulosum of the dentate gyrus among experimental

mice 1 day, 7, 120 days and 15 months after irradiation with 5Gy at P3 indicated a significant change of the number of γ H2AX foci ($P < 0.001$ by One-way analysis of variance (ANOVA)). Student's t-test showed a significant reduction of γ H2AX foci from 1 day, 7 days to 120 days ($P < 0.05$, by a Student's t-test). However, no significant change in the number of γ H2AX foci was observed from 120 day to 15 months after irradiation ($P > 0.05$) (Figure 5).

The number of γ H2AX foci in the stratum granulosum of the dentate gyrus among experimental mice 1 day, 7, 120 days and 15 months after irradiation with 5Gy at P10 was also changed significantly ($P < 0.01$ by One-way ANOVA). Student's t-test showed no significant difference in the number of γ -H2AX foci between 1 day and 7 days after irradiation at P10 ($P > 0.05$), the number of γ -H2AX foci decreased significantly at 120 days after irradiation at P10 when compared to those at P1 and P7 day(s) after irradiation ($P < 0.01$). From 120 days to 15 months after irradiation, the number of γ -H2AX foci in the stratum granulosum did not change significantly. There was also a significant change in the number of γ -H2AX foci in the stratum granulosum of the dentate gyrus among experimental mice 1 day, 7, 120 days and 15 months after irradiation with 5Gy at P21 ($P < 0.05$ by One-way ANOVA). From 1 day to 7 days after irradiation at P21, the number of γ -H2AX foci increased significantly ($P < 0.5\%$). However, no

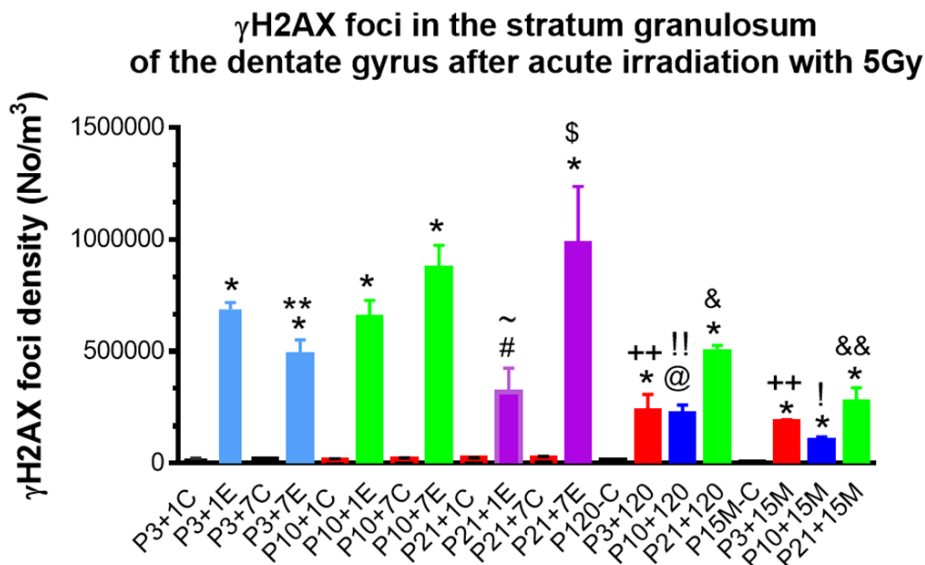


Figure 5. Quantitative analysis of γ H2AX foci in the stratum granulosum of the dentate gyrus among experimental mice 1day, 7, 120 days and 15 months after irradiation with 5Gy at P3, P10 and P21 respectively. * $P < 0.001$; @ $P < 0.01$ # $P < 0.05$ compared to the age-matched control, & $P < 0.01$ compared to P3+120 or P10+120; \$ $P < 0.05$ compared to P21+1E; ~ $P < 0.05$ compared to P3+1E, P10+1E; ** $P < 0.05$ compared to P3+1E and P3+7E; ++ $P < 0.001$ compared to P3+1E; !! $P = 0.001$ compared to P10+1E; ! $P < 0.01$ compared to P10+1E; && $P < 0.05$ compared to P21+120. C: Control, E: Experimental.

Table 1. γ -H2AX foci in the mouse brain at 1, 7, 120 days and 15 months after the acute irradiation at P3, P10 and P21.

| γ -H2AX | Neurogenesis and migration | | | | Hippocampus | | | | | Cortex | | | Stri | Thal | BV | CC/EC |
|----------------|----------------------------|-----|-----|-------|--------------------|-----|-----|-------|--------|--------|-------|------|------|------|-----|-------|
| | SVZ | RMS | OB | Hilus | Dentate gyrus (DG) | | | CA1-3 | | I | II-IV | V-VI | | | | |
| | | | | | SG | SM | SO | SP | SR-SLM | | | | | | | |
| P3+1 C | +/- | +/- | +/- | +/- | +/- | +/- | +/- | +/- | +/- | +/- | +/- | +/- | +/- | +/- | +/- | +/- |
| P3+1 E | +++ | +++ | +++ | +++ | +++ | +++ | +++ | +++ | +++ | +++ | +++ | +++ | +++ | +++ | +++ | +++ |
| P3+7 C | +/- | +/- | +/- | +/- | +/- | +/- | +/- | +/- | +/- | +/- | +/- | +/- | +/- | +/- | +/- | +/- |
| P3+7 E | +++ | +++ | +++ | +++ | +++ | +/- | +/- | +++ | +/- | +++ | +++ | +++ | +++ | +++ | +/- | +/- |
| P10+1 C | +/- | +/- | +/- | +/- | +/- | +/- | +/- | +/- | +/- | +/- | +/- | +/- | +/- | +/- | +/- | +/- |
| P10+1 E | +++ | + | +++ | +++ | +++ | +/- | +/- | +++ | +/- | +/- | +++ | +++ | +++ | +++ | +/- | +/- |
| P10+7 C | +/- | +/- | +/- | +/- | +/- | +/- | +/- | +/- | +/- | +/- | +/- | +/- | +/- | +/- | +/- | +/- |
| P10+7 E | ++ | +/- | +++ | +++ | +++ | +/- | +/- | +++ | +/- | +/- | +++ | +++ | +++ | +++ | +/- | +/- |
| P21+1 C | +/- | +/- | +/- | +/- | +/- | +/- | +/- | +/- | +/- | +/- | +/- | +/- | +/- | +/- | +/- | +/- |
| P21+1 E | + | + | +++ | ++ | +++ | +/- | +/- | +++ | +/- | +/- | +++ | + | +++ | +++ | +/- | +/- |
| P21+7 C | +/- | +/- | +/- | +/- | +/- | +/- | +/- | +/- | +/- | +/- | +/- | +/- | +/- | +/- | +/- | +/- |
| P21+7 E | + | + | +++ | +++ | +++ | +/- | +/- | +++ | +/- | +/- | +++ | +++ | +++ | +++ | +/- | +/- |
| P+120C | +/- | +/- | +/- | +/- | +/- | +/- | +/- | +/- | +/- | +/- | +/- | +/- | +/- | +/- | +/- | +/- |
| P3+120 | + | + | + | +/- | +++ | +/- | +/- | +++ | +/- | +/- | ++ | + | +++ | + | +/- | +/- |
| P10+120 | + | + | + | +/- | +++ | +/- | +/- | +++ | +/- | +/- | ++ | ++ | +++ | + | +/- | +/- |
| P21+120 | + | + | + | +/- | +++ | +/- | +/- | +++ | +/- | +/- | ++ | ++ | +++ | + | +/- | +/- |
| MRI-P15M-C | +/- | +/- | +/- | +/- | +/- | +/- | +/- | +/- | +/- | +/- | +/- | +/- | +/- | +/- | +/- | +/- |
| MRI-P3+15M | + | + | + | +/- | ++ | +/- | +/- | + | +/- | +/- | + | + | + | + | +/- | +/- |
| MRI-10+15M | + | + | + | +/- | ++ | +/- | +/- | ++ | +/- | +/- | ++ | ++ | ++ | ++ | +/- | +/- |
| MRI-21+15M | + | +++ | +++ | +/- | +++ | +/- | +/- | +++ | +/- | +/- | +++ | +++ | +++ | +++ | +/- | +/- |

BV: Blood Vessel; CC: corpus callosum; EC: Ependymal cells; OB: olfactory bulb; RMS: rostral migratory stream; SM: Stratum moleculare; SG: stratum granulosum; SP: stratum pyramidale; SR-SLM: Stratum radiatum and stratum laculosum moleculare; Stri: striatum; SVZ: subventricular zone; Thal: Thalamus; Per screen size under 400x for counting γ -H2AX foci: 310 μ m x 230 μ m; per screen foci: +++: > 10 foci; ++: 5-10 foci; +: 2-5 foci; +/-: 0< γ -H2AX<2. C: Control, E: Experimental.

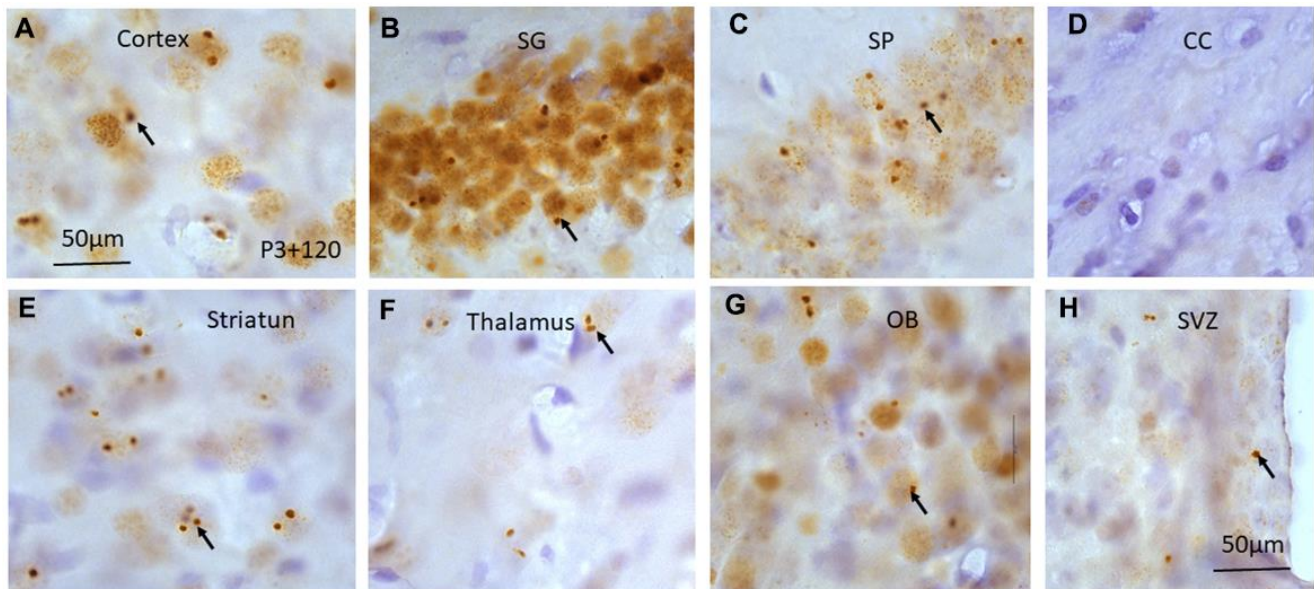


Figure 6. γ H2AX immunostaining counterstained with hematoxylin shows irradiation-induced γ H2AX foci (arrows) in different brain regions including cortex (A), stratum granulosum of the dentate gyrus (B), stratum pyramidale of CA1 area of the hippocampus (C), corpus callosum (CC) (D), striatum (E), thalamus (F), olfactory bulb (G) and subventricular zone of the lateral ventricle (H) at 120 days after irradiation at P3. Scan bar=50 μ m in (A) applies to (B–H).

difference in the number of γ -H2AX foci in the stratum granulosum at 120 days after irradiation at P21 when compared to those at P1 and P7 day(s) ($P>0.05$). A significant reduction of γ -H2AX foci in the stratum granulosum from 120 days to 15 months occurred ($P<0.05$) (Figure 5).

The number of γ -H2AX foci in the stratum granulosum of the dentate gyrus among experimental mice 1 day after irradiation with 5 Gy at P3, P10 and P21 was also changed significantly ($P<0.01$ by One-way ANOVA). Student's *t*-test showed no significant difference in the number of γ -H2AX foci at 1 day after irradiation at P3 and P10 ($P>0.05$). However, a significant reduction of the number of γ -H2AX foci occurred at 1 day after irradiation at P21 when compared to those at P3 and P10 respectively ($P<0.05$) (Figure 5).

From 120 days to 15M after irradiation at P3 and P10, no significant change of γ -H2AX foci in the stratum granulosum of the dentate gyrus was observed ($P>0.05$). However, a significant reduction of γ -H2AX foci from 120 days to 15M was found after irradiation at P21 ($P<0.05$) (Figure 5).

Survival analysis

The long-term monitoring of 7 control, 9 P3, 7 P10, and 5 P21 irradiated mice indicated that only 1 control mouse (14%) died before the age of 13 months. However, 5 P3 (56%), 4 P10 (57%) and 2 P21 (40%)

irradiated mice died before 13 months after irradiation. This finding suggested that radiation-induced brain aging indicated by γ -H2AX foci (or PDDF) may be related to shorter life expectancy in irradiated mice.

DISCUSSION

The novel findings of this study include: 1) Acute irradiation with 5Gy induced γ H2AX foci in the epithelial cells in pia mater, glial cells and blood vessel endothelial cells in the brain of mice 1 day after radiation exposure at P3, but not at P10 and P21. It suggested a drastic difference in radiosensitivity of these cells between P3 and P10 or P21 mice. Irradiation at P10 and P21 induced γ H2AX foci in neurons in all brain regions at 1, 7, 120 day(s) and 15 months after irradiation with 5Gy, which was similar to those mice 7, 120 day(s) and 15 months after radiation exposure with 5Gy at P3. 2) radiation-induced γ H2AX foci are mainly localized in brain neurons and persisted until the later stages (15 months after irradiation) of animal life, this PDDF may be related to the brain aging as experimental mice with PDDF died earlier than the control mice.

Radiosensitivity of different cell types in P3, P10 or P21 mouse brain

Brain insults such as radiation exposure during critical early life stages may induce different neuropathological changes which last a lifetime, leading to the

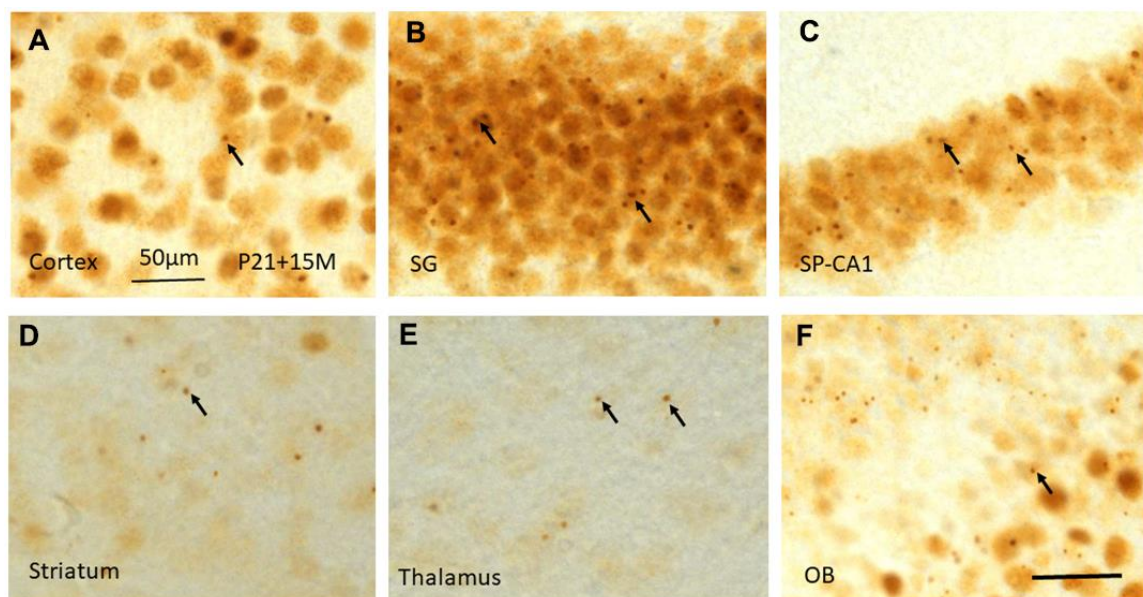


Figure 7. γ H2AX immunostaining shows irradiation-induced γ H2AX foci (arrows) in different brain regions including cortex (A), stratum granulosum of the dentate gyrus (B), stratum pyramidale of CA1 area of the hippocampus (C), striatum (D), thalamus (E), and olfactory bulb (F) at 15 months after irradiation at P21. Scan bar=50 μ m in (A) applies to (B–F).

development of different brain disorders including schizophrenia [18, 19], dementia [20], depression [13], seizure [21], Alzheimer's disease [17]. The immature brain is more radiosensitive than mature one due to more neurogenesis. A number of previous studies have suggested that P10 represents the most sensitive day to different toxins including radiation exposure [22–24]. P10 mice have therefore been used to establish different brain insult models such as radiation exposure [22–24], ibotenic acid excitotoxic brain insult [25], hypoxia-ischemia [26, 27], hypoxic-ischemic encephalopathy [28]. In the present study, we showed that the epithelial cells in pia mater, endothelial cells of cerebral blood vessel and glial cells in corpus callosum in P3 mouse brain was more radiosensitive than P10 and P21 at 1 day after γ -radiation exposure with 5Gy. In the hippocampus, γ H2AX foci were localized not only in principal cell layers, i.e., stratum pyramidale of CA1-3 areas and stratum granulosum, but also in the non-principal cell layers, i.e., in the strata lacunosum moleculare, radiatum, and oriens of CA1-3 areas, in the stratum moleculare and hilus of the dentate gyrus 1 day after radiation exposure at P3. It suggested that γ -H2AX foci may be localized in the glial cells, cells in blood vessel and interneurons in addition to principal neurons such as pyramidal neurons in CA1-3 areas and granule cells in the dentate gyrus. The similar γ -H2AX foci in the non-principal cell layers were not observed 1 day after irradiation at P10 and P21. These observations indicate a significantly greater radiosensitivity of P3 mouse brain than P10 and P21.

At 1 day after irradiation of P3, P10 and P21 mice, there was no difference in number of γ H2AX in the stratum granulosum of the dentate gyrus between P3 and P10 mice. Much fewer γ H2AX foci were observed at P21 when compared to P3 or P10 mice. It suggested that P21 mouse granule cells may be less radiosensitive than P3 and P10. It is in agreement with the result indicating that granule cells in P21 mice expressed calbindin but not calretinin. The former is a mature neuronal marker whereas the latter is an immature granule cell marker [29].

A significant reduction of γ H2AX foci in the stratum granulosum from 1 day, 7 to 120 days after irradiation at P3 suggested that radiation-induced DNA repair in the brain occurred continuously during these periods. However, the number of γ H2AX foci did not reduce from 120 day to 15 months after radiation exposure. It suggests that with aging, radiation-induced DNA repair may become much slower, inefficient or even cease during this period. No significant reduction in the number of γ H2AX foci from 1 day and 7 days, but a significant decrease at 120 days after irradiation at P10 compared to those at P1 and P7 day(s) after irradiation,

it suggests that DNA repair may not be effective at early days after irradiation and granule cells may take long time to recover. On the contrary, a drastic increment in the number of γ H2AX foci from 1 day to 7 days after irradiation at P21 suggested a possible delayed DNA damage and repair during this period. The different DNA repair responses indicated by γ H2AX foci 1 to 7 days after radiation exposure at P3, P10 and P21 may indicate a significantly higher radiosensitivity of granule cells in earlier postnatal day mice, leading to more neuronal death and less surviving γ H2AX immunopositive cells. However, the number of γ H2AX foci in the stratum granulosum did not change among mice 1, 7 and 120 days after irradiation at P21 thereby suggesting that radiation-induced DNA repair in the stratum granulosum of P21 mice may occur mainly at early stage within 24 h post-irradiation. A significant reduction of γ H2AX foci in the stratum granulosum from 120 days to 15 months suggested a possibly delayed DNA repair when animals were irradiated at P21. Further study may be needed to elucidate the mechanism of such a delayed DNA repair in P21 mice.

A previous study has indicated that a complete DNA repair occurred 24 h after prenatal γ - irradiation with 2 Gy at 14.5 day of gestation [30]. The presence of PDDF in the neurons of the brain in the present study suggested that further investigation is still needed to determine whether prenatal brain neurons have a high capability to self-repair or γ H2AX foci still exist in the brain of animals at different postnatal stages of the animal life. A complete lost γ H2AX foci was also observed in surviving neural precursor cells within 24h after irradiation [31], it is supported by our study showing the presence of γ H2AX foci in the stratum granulosum, but not in the subgranular zone of dentate gyrus. However, it was inconsistent with report by Barral et al. who indicated that γ H2AX in the neurogenetic regions such as subventricular zone (SVZ) of telencephalon and the cerebellar cortex was related to the fate of neuronal precursors in the adult animals [5].

Radiation-induced γ H2AX in the cerebrovascular system, hippocampal interneurons, the corpus callosum (CC) and pia mater

Induced γ H2AX in the cerebrovascular system

In vitro study of γ -irradiation-induced endothelial cell DNA damage, apoptosis, senescence and relevant molecular mechanisms have been well documented [32–38]. However, *in vivo* investigation of radiation-induced age-dependent DNA damages in endothelial cells of brain capillary is scarce, in particular, irradiation at different early postnatal days. *In vivo* study in the young adult rat (7-8- week-old) demonstrated abnormal changes in the blood-brain

barrier (BBB) and leukocyte-endothelial cell interactions in the blood vessel in pia mater after cranial irradiation with 20Gy [39]. Acute cranial irradiation of P14 mice with 10 Gy enhanced the ratio of endothelial cells to the control in different brain regions suggesting that brain endothelial cells were more radio-resistant than other cells. It was in agreement with the finding that no significant change in *Smpd1* gene from 6 h to 7 days after radiation exposure [37]. Radiation exposure with 8Gy transiently affected the hippocampal neurovascular niche in the immature brain from 6h to 1 day after irradiation [40], and there was a significant decrease in the total number of microvessels as well as the branching points from 1 to 7 weeks after radiation exposure. However, the microvessel densities were normalized with time thereafter. It suggested that from a long-term point view, radiation exposure may not affect angiogenesis of immature mouse brain [41]. Peroxisome proliferator-activated receptor gamma coactivator 1 alpha (*PGC1 α*) is a regulator of cellular mitochondrial function and a transcriptional activator of mitochondria-related genes. It negatively regulates vascular senescence by activating reactive oxygen species detoxification and increasing the number of mitochondria [33, 42]. Radiation-induced *PGC1 α* acetylation may be related to mitochondrial dysfunction leading to cellular senescence and aging [43]. Interestingly, irradiation of P11 rats with 6Gy induced BBB damage and reduced blood flow in the cerebellum much more than other brain regions after irradiation [44]. In the present study, γ H2AX foci were observed in the endothelial cells of brain capillary 1 day, but not 7 and 120 days after irradiation with 5Gy in P3 mice, but not P10 and P21 mice. It suggested that the endothelial cells of brain capillary of P3 mice are more radio-sensitive than P10 and P21 mice. The disappearance of γ H2AX foci at 7 days after irradiation indicated that DNA repair process in the capillary endothelial cells might have already completed. Overall, irradiation with 5Gy may induce transient DNA damage in capillary endothelial cells in P3 mice, but may not significantly affect brain capillary in P10 and P21 mice.

γ H2AX expression in the hippocampal interneurons, the corpus callosum and pia mater

Accumulated data indicate that gamma-aminobutyric acid immunopositive interneurons are more radiosensitive than principal cells in the cortex, hippocampus, or retina after pre- or post-natal radiation exposure [45–51]. While acute radiation exposure with 6Gy to P11 rat did not affect the inhibitory network of parvalbumin interneurons in the dentate gyrus although it completely ablated neurogenesis in the subgranular zone [52]. However, acute or fractionated X-irradiation with a total

of 2 to 20 Gy to mice induced a significant reduction of parvalbumin interneurons in the subgranular zone of the dentate gyrus [48–50]. Neonatal and adolescent brain insults may induce cognitive deficits and increased risk of mental illnesses, including depression, bipolar disorder, autism, epilepsy and schizophrenia. Loss of hippocampal parvalbumin interneurons may be involved in neuropathological changes of these disorders [53, 54]. In the present study, the appearance of γ H2AX foci in non-principal cell layers of the hippocampus 1 day after irradiation with 5Gy in P3 mice suggested their possible cellular localization in the hippocampal interneurons and glial cells which is supported by hematoxylin counterstaining.

A number of previous studies have shown the decreased number of oligodendrocytes in the CC [55], increased density of astrocytes [56] and strongly induced inflammation-related genes such as C-C Motif Chemokine Ligand 2 (*CCL2*), *CCL11* and *IL6* [37] 120 after brain irradiation with 8 Gy to P14 mice. In the present study, the appearance of γ H2AX foci in the corpus callosum 1 day after irradiation with 5Gy in P3 mice may suggest the cellular localization of γ H2AX foci in oligodendrocytes. Moreover, an increased proliferation of astrocytes and neuroinflammation may support that irradiation with 5Gy may activate both astrocyte and microglia to proliferation, but not induce DNA damage or γ H2AX foci in the two types of glial cells. The appearance of γ H2AX foci in the pia mater at 1 day after irradiation with 5Gy at P3 suggested extensive DNA damage in epithelial cells.

γ H2AX and apoptosis

Phosphorylation of H2AX is linked not only to a DNA damage response, but also to chromatin remodelling and apoptotic DNA fragmentation [57]. Radiation-induced upregulation of pro-apoptotic genes and delayed DNA lesions in testicular cells suggests that delayed DNA lesions may be related to an active apoptotic process [58]. In neurons of prenatal radiation exposed brain, the apoptosis was related to phosphorylation and subsequent degradation of γ H2AX in the course of DNA fragmentation during apoptosis [30]. The insult of a lymphocyte cell line induces γ H2AX expression. However, the induction is prevented by apoptosis inhibitor, suggesting that γ H2AX expression occurs subsequent to apoptosis [59]. In the present study, no co-localization of γ H2AX foci with apoptotic bodies at 1 day after irradiation at different postnatal days. Combined with the previous study showing that initiation of DNA fragmentation during apoptosis results in γ H2AX expression [60]. it suggests that unrepaired DNA damage or γ H2AX foci at the early stages (maybe first a few hours) after irradiation with

5Gy may be related to the formation of apoptotic bodies in the mouse brain.

Transient DNA damage foci or PDDF, aging, neurological, neuropsychological and genetic disorders

Transient expression of γ H2AX has been considered as an early biomarker of neuronal endangerment after different brain insults such as glutamate receptor-dependent excitotoxicity [7, 61], seizures [8], cellular senescence [11, 62], ischemia [63], ethanol [64, 65] and radiation exposures [12, 66, 67] and genotoxic stress [68]. Some of γ H2AX foci may exist in neurons as PDDF for a long period of time as shown at 15 months after irradiation in the present study. PDDF and DNA damage response (DDR) signalling are responsible for inflammatory cytokine secretion. Upregulation of PDDF and secreted IL6 occur in p53 deficient cells [69], which is causally involved in cellular senescence and organismal aging [70]. The presence of PDDF in neurons in different brain regions and shortened life expectancy after radiation exposure at P3, P10 and P21 suggested that radiation-induced brain aging may be related to the earlier death of irradiated mice. Radiation-induced PDDF also occurred in other cell models. In MRC-5 cells, X-irradiation-induced γ H2AX foci remained for 2 weeks suggesting an unrejoined DNA double-strand breaks [71]. The accumulation of PDDF of checkpoint factors may induce G1 arrest leading to tumor suppression to permanently exclude cells with remaining DNA damage [72]. We therefore speculate that the localization of PDDF in neurons may explain why radiation-induced brain tumor is mainly glia but not neuronal originated. In normal human diploid fibroblasts, X-irradiation induced transient γ H2AX foci formation which disappeared rapidly. The remaining foci clustered along the chromosomal bridges 96 h after irradiation, and might be an aberrant chromatin structure by illegitimate rejoining. Large γ H2AX foci continuously amplify DNA damage signal leading to an irreversible growth arrest [73–75]. In non-proliferating human mammary epithelial cells, iron-ion irradiation-induced PDDF may be related to limited availability of double-strand break (DSB) repair pathways in G0/G1-phase [76]. The increase in the size of individual foci may be due to the spreading of γ H2AX over a large chromatin domain leading to the accumulation of a multitude of DNA damage response proteins distal to the lesion [77].

The defective DNA repair in neurons with accumulation of PDDF and loss of genome integrity may contribute to aging and many neurodegenerative disorders such as amyotrophic lateral sclerosis (ALS), Parkinson's disease (PD), AD and Huntington's disease (HD). In lumbar

motor neurons from ALS patients, a significant up-regulation of γ H2AX, phosphorylated ataxia telangiectasia mutated (p-ATM), cleaved poly (ADP-Ribose) polymerase 1 (PARP-1) and tumour suppressor p53-binding protein (53BP1) was observed [78]. Intracellular accumulation of α -synuclein (α -syn) is a hallmark of synucleinopathies, including PD. Exogenous addition of preformed α -syn fibrils (PFFs) into primary hippocampal neurons induced α -syn aggregation and accumulation and increased H2AX Ser139 phosphorylation, suggesting that γ H2AX may play a role in α -syn induced pathogenesis of PD [79]. Failure to engage the repair system and initiate repair after DNA damage is likely a key mechanism for determining early damage in the hippocampus of AD [80]. L5, a human plasma low-density lipoprotein (LDL), fraction induces cell damage by activating ATM/H2AX-associated DNA breakage pathway and apoptosis via lectin-like oxidized LDL receptor-1 (LOX-1) signalling to p53, leading to cleavage of caspase-3, and to the development of neurodegenerative diseases including AD [81]. However, no correlation between persistent γ H2AX foci and apoptosis after irradiation with high-dose synchrotron-generated microbeams in cultured normal human fibroblasts and p53 wild-type malignant glioma cells may suggest the importance of non-apoptotic responses such as p53-mediated growth arrest or premature senescence [82].

Increased levels of γ H2AX occurred not only in astrocyte [9] and neuronal [83] nuclei, but also in blood lymphocytes of AD patients, suggesting that lymphocyte γ H2AX levels may be used to identify population with a high risk of AD development [84]. Increased proportions of γ H2AX-labeled neurons and astrocytes in the hippocampus and frontal cortex of mild cognitive impairment (MCI) and AD patients also suggested that there might exist a causal relationship between the early neuronal accumulation of DSB and neurodegenerative disorders including HD [10] and cognitive impairment [85]. Increased γ H2AX, Checkpoint kinase 2 (*Chk2*) protein phosphorylation, p53 were also reported in Down syndrome (DS) fibroblasts from both fetal and adult donors during unperturbed growth conditions [86], in the hippocampal neurons up to 14 days after laparotomy in elderly mice [87]. γ H2AX may also be used as a reliable marker of gene silencing in DNA damaged neuron as unrepaired DNA in neurons is sequestered in discrete PDDF of transcriptionally silent chromatin which is essential to preserve genome stability and prevent the synthesis of aberrant mRNA and protein products encoded by damaged genes [88, 89].

At molecular level, inhibition of glycogen synthase kinase 3 β (GSK3 β) accelerated DSB repair efficiency

in irradiated mouse hippocampal neurons, which coincided with attenuation of irradiation-induced γ H2AX foci. It suggested that GSK3 β inhibitors might be promising radio-neuro-protectants [90]. Radiation-induced expression of pro-survival and DNA repair proteins such as γ H2AX and 53BP1, and DNA repair capacities are negatively regulated by Sirtuin 2 (SIRT2) leading to cell death and DNA damage [91].

Concluding remarks

Extensive γ H2AX foci were induced in the mouse brain at 1 day after irradiation at P3, P10 and P21, which lasted till 15 months after irradiation. The appearance of γ H2AX foci in the epithelial cells in pia mater, glial cells and blood vessel endothelial cells in the brain of mice 1 day after irradiation at P3, but not P10 and P21 suggested that P3 mouse brain is much more radiosensitive than P10 and P21. The early life radiation-induced γ H2AX foci, or PDDF may be involved in the brain aging leading to the shortened life expectancy in irradiated animals. From a speculative point of view, PDDF may be involved in the radiation-induced progressive neuronal loss, and the onset of different neurological and neuropsychological disorders depending on the patterns of neuropathological changes. It may also represent gene silencing in DNA damaged neuron to preserve genome stability and prevent the synthesis of aberrant mRNA and protein products as suggested previously [70, 88, 89].

MATERIALS AND METHODS

Animal irradiation

A total of 80 mice (5 in each control and experimental groups) was used for short- to mid-term study at 1 (5xP3+1 control; 5xP3+1 experimental; 5xP10+1 control; 5xP10+1 experimental; 5xP21+1 control; 5xP21+1 experimental), 7(5xP3+7 control; 5xP3+7 experimental; 5xP10+7 control; 5xP10+7 experimental; 5xP21+7 control; 5xP21+7 experimental) and 120 (5xP120-control; 5xP3+120 experimental; 5xP10+120 experimental; 5xP21+120 experimental) days after radiation exposure. To monitor long-term (15 months) effect of acute radiation exposure and brain γ H2AX and ageing, 28 mice, i.e., 7 control (including 3 P3, 2 P10 and 2 P21), 21 experimental (including 9 P3, 7 P10, and 5 P21) mice were used. The animals were irradiated according to the same protocol in our previous studies [92]. In brief, freely moving mice at postnatal day 3 (P3), P10 and P21 were whole body γ -irradiated with 5 Gy (3.33Gy/m). We chose 5Gy because with this dose, impairment of neurogenesis could be consistently induced but there is no mortality in Balb/c mice [48, 49, 51, 92]. Animals were euthanized with a mixture of

ketamine (75mg/kg) and medetomidine (1mg/kg) at 0.1ml/10g 1, 7, 120 day(s), and 15 months after irradiation, and perfused with 4% paraformaldehyde. The mouse brain was removed, post-fixed overnight, and then transferred to 30% sucrose in 0.1M phosphate buffer (PB) (pH: 7.4). All the animal experimental protocols were approved by the Institutional Animal Care and Use Committee (IACUC) of National University of Singapore (R15-1576). In addition, consistent efforts were made to minimize animal suffering and to use the minimal number of animals throughout the study.

Immunohistochemical staining

Immunohistochemical staining was done according to our previous studies [92]. Sagittal brain sections at 40 μ m were blocked with 3% H₂O₂ and then 4% normal goat serum at room temperature. The sections were incubated with primary rabbit antibody for γ H2AX (1:200) (Cell Signaling Technology, Inc., MA, Danvers, USA) and then placed in goat anti-rabbit secondary antibody for 1 hour. The sections were placed in avidin-biotin complex (ABC) reagent (Vector Laboratories Inc., Burlingame, CA, USA) for 1 h, then reacted in 3,3'-diaminobenzidine (DAB) Peroxidase Substrate (Vector Laboratories Inc., Burlingame, CA, USA) for 10 minutes. The sections were mounted, covered and the images were then taken under microscopy (Leica Microsystems GmbH, Wetzlar, Germany).

Hematoxylin counterstaining

To further analyse cellular localization of γ H2AX foci at 1, 7 and 120 day(s) after irradiation at P3, P10 and P21 respectively, coverslip was removed after stereological analysis by immersing slides in sequence in Histo-Clear, 100%, 95%, 75%, 50%, 25% ethanol, and then in ultrapure water. The sections were then counterstained with hematoxylin and covered with coverslip.

Statistical analysis

For unbiased counting of γ H2AX foci in the stratum granulosum of the dentate gyrus, the Stereologer from Stereology Resource Center Biosciences, Inc. (SRC Biosciences, Florida, USA) was used. Three (P3+1, P3+7, P10+1, P10+7) to six (P21+1, P21+7, P120-control P3+120, P10+120, P21+120, P15M-control, P3+15M, P10+15M, P21+15M) brain sections from individual mouse were counted. γ H2AX foci were counted at 400 \times , and indicated as the number of foci/mm³ in the stratum granulosum of the dentate gyrus. All the data were then analyzed by one-way ANOVA followed by student's t-test. Statistical significance was considered at P<0.05.

Abbreviations

ABC: Avidin–biotin complex; AD: Alzheimer's disease; ALS: Amyotrophic lateral sclerosis; ANOVA: Analysis of variance; α -syn: α -synuclein; 53BP1: p53 binding protein 1; BRCA1: Breast cancer susceptibility gene 1; CC: Corpus callosum; CCL: C-C Motif Chemokine Ligand ; Chk2: Checkpoint kinase 2; CSPall: Central subpallium/classic basal ganglia; DAB: 3,3'-Diaminobenzidine; DPall: Dorsal pallium; DSB: Double-strand break; γ H2AX: Gamma H2A histone family member X; GSK3 β : Glycogen synthase kinase 3 β ; IACUC: Institutional Animal Care and Use Committee; LDL: Low-density lipoprotein; MCI: Mild cognitive impairment; MPall: Medial pallium; P3: postnatal day 3; P10: postnatal day 10; P21: postnatal day 21; PB: Phosphate buffer; PBS: Phosphate buffer saline; PBS-TX: Phosphate buffer saline with 0.1% Triton X-100; PD: Parkinson's disease; PDDF: Persistent DNA damage foci; PGC1 α : Peroxisome proliferator–activated receptor gamma coactivator 1 alpha; RMS: Rostral migratory streams; ROS: reactive oxygen species; SGZ: Subgranular zone; SIRT2: Sirtuin 2; SVZ: Subventricular zone; TelA: Alar plate of evaginated telencephalic vesicle; TMS: Temporal migratory streams.

AUTHOR CONTRIBUTIONS

FRT conceptualized, designed the study, performed experiments, data analysis and wrote the paper. LL performed experiments, data analysis and wrote the paper. HW, KH performed experiments, GS critically review the manuscript. FRT and GS obtained the funding. The technical support from Dr Hongyuan Shen, Ms Renu Chandra Segaran, Ms Li Yun Chan from the Singapore Nuclear Research and Safety Initiative; Mrs Lu Fan, Department of Pharmacology, National University of Singapore and Mr Zijun Wu from the Yangtze University China is also greatly appreciated.

CONFLICTS OF INTEREST

The authors declare that they have no conflicts of interest.

FUNDING

This research was funded by the National Research Foundation (NRF) of Singapore to Singapore Nuclear Research and Safety Initiative (FRT, GS) and the Health Commission of Hubei Province scientific research project (NO.WJ2021Q015) to LL.

REFERENCES

1. Rothkamm K, Horn S, Scherthan H, Rössler U, De Amicis A, Barnard S, Kulka U, Lista F, Meineke V, Braselmann H, Beinke C, Abend M. Laboratory intercomparison on the γ -H2AX foci assay. *Radiat Res.* 2013; 180:149–55.
<https://doi.org/10.1667/RR3238.1>
PMID:[23883318](https://pubmed.ncbi.nlm.nih.gov/23883318/)
2. Redon CE, Nakamura AJ, Gouliava K, Rahman A, Blakely WF, Bonner WM. The use of gamma-H2AX as a biodosimeter for total-body radiation exposure in non-human primates. *PLoS One.* 2010; 5:e15544.
<https://doi.org/10.1371/journal.pone.0015544>
PMID:[21124906](https://pubmed.ncbi.nlm.nih.gov/21124906/)
3. d'Adda di Fagagna F, Reaper PM, Clay-Farrace L, Fiegler H, Carr P, Von Zglinicki T, Saretzki G, Carter NP, Jackson SP. A DNA damage checkpoint response in telomere-initiated senescence. *Nature.* 2003; 426:194–98.
<https://doi.org/10.1038/nature02118>
PMID:[14608368](https://pubmed.ncbi.nlm.nih.gov/14608368/)
4. Sedelnikova OA, Horikawa I, Zimonjic DB, Popescu NC, Bonner WM, Barrett JC. Senescing human cells and ageing mice accumulate DNA lesions with unrepairable double-strand breaks. *Nat Cell Biol.* 2004; 6:168–70.
<https://doi.org/10.1038/ncb1095>
PMID:[14755273](https://pubmed.ncbi.nlm.nih.gov/14755273/)
5. Barral S, Beltramo R, Salio C, Aimar P, Lossi L, Merighi A. Phosphorylation of histone H2AX in the mouse brain from development to senescence. *Int J Mol Sci.* 2014; 15:1554–73.
<https://doi.org/10.3390/ijms15011554>
PMID:[24451138](https://pubmed.ncbi.nlm.nih.gov/24451138/)
6. Turinetto V, Giachino C. Histone variants as emerging regulators of embryonic stem cell identity. *Epigenetics.* 2015; 10:563–73.
<https://doi.org/10.1080/15592294.2015.1053682>
PMID:[26114724](https://pubmed.ncbi.nlm.nih.gov/26114724/)
7. Crowe SL, Movsesyan VA, Jorgensen TJ, Kondratyev A. Rapid phosphorylation of histone H2A.X following ionotropic glutamate receptor activation. *Eur J Neurosci.* 2006; 23:2351–61.
<https://doi.org/10.1111/j.1460-9568.2006.04768.x>
PMID:[16706843](https://pubmed.ncbi.nlm.nih.gov/16706843/)
8. Crowe SL, Tsukerman S, Gale K, Jorgensen TJ, Kondratyev AD. Phosphorylation of histone H2A.X as an early marker of neuronal endangerment following seizures in the adult rat brain. *J Neurosci.* 2011; 31:7648–56.
<https://doi.org/10.1523/JNEUROSCI.0092-11.2011>
PMID:[21613478](https://pubmed.ncbi.nlm.nih.gov/21613478/)
9. Myung NH, Zhu X, Kruman II, Castellani RJ, Petersen RB, Siedlak SL, Perry G, Smith MA, Lee HG. Evidence of DNA damage in Alzheimer disease: phosphorylation of histone H2AX in astrocytes. *Age (Dordr).* 2008; 30:209–15.

- <https://doi.org/10.1007/s11357-008-9050-7>
PMID:[19424844](https://pubmed.ncbi.nlm.nih.gov/19424844/)
10. Jeon GS, Kim KY, Hwang YJ, Jung MK, An S, Ouchi M, Ouchi T, Kowall N, Lee J, Ryu H. Deregulation of BRCA1 leads to impaired spatiotemporal dynamics of γ -H2AX and DNA damage responses in Huntington's disease. *Mol Neurobiol*. 2012; 45:550–63.
<https://doi.org/10.1007/s12035-012-8274-9>
PMID:[22580959](https://pubmed.ncbi.nlm.nih.gov/22580959/)
 11. He ZY, Wang WY, Hu WY, Yang L, Li Y, Zhang WY, Yang YS, Liu SC, Zhang FL, Mei R, Xing D, Xiao ZC, Zhang M. Gamma-H2AX upregulation caused by Wip1 deficiency increases depression-related cellular senescence in hippocampus. *Sci Rep*. 2016; 6:34558.
<https://doi.org/10.1038/srep34558>
PMID:[27686532](https://pubmed.ncbi.nlm.nih.gov/27686532/)
 12. Das A, McDonald DG, Dixon-Mah YN, Jacqmin DJ, Samant VN, Vandergrift WA 3rd, Lindhorst SM, Cachia D, Varma AK, Vanek KN, Banik NL, Jenrette JM 3rd, Raizer JJ, et al. RIP1 and RIP3 complex regulates radiation-induced programmed necrosis in glioblastoma. *Tumour Biol*. 2016; 37:7525–34.
<https://doi.org/10.1007/s13277-015-4621-6>
PMID:[26684801](https://pubmed.ncbi.nlm.nih.gov/26684801/)
 13. Loganovsky K, Havenaar JM, Tintle NL, Guey LT, Kotov R, Bromet EJ. The mental health of clean-up workers 18 years after the Chernobyl accident. *Psychol Med*. 2008; 38:481–88.
<https://doi.org/10.1017/S0033291707002371>
PMID:[18047772](https://pubmed.ncbi.nlm.nih.gov/18047772/)
 14. Loganovsky KN, Vasilenko ZL. Depression and ionizing radiation. *Probl Radiac Med Radiobiol*. 2013; 18: 200–19.
PMID:[25191725](https://pubmed.ncbi.nlm.nih.gov/25191725/)
 15. Segaran RC, Chan LY, Wang H, Sethi G, Tang FR. Neuronal Development-Related miRNAs as Biomarkers for Alzheimer's Disease, Depression, Schizophrenia and Ionizing Radiation Exposure. *Curr Med Chem*. 2021; 28:19–52.
<https://doi.org/10.2174/0929867327666200121122910> PMID:[31965936](https://pubmed.ncbi.nlm.nih.gov/31965936/)
 16. Hong JS, Tian J, Han QF, Ni QY. Quality of life of nasopharyngeal cancer survivors in China. *Curr Oncol*. 2015; 22:e142–47.
<https://doi.org/10.3747/co.22.2323> PMID:[26089724](https://pubmed.ncbi.nlm.nih.gov/26089724/)
 17. Lehrer S, Rheinstein PH, Rosenzweig KE. Association of Radon Background and Total Background Ionizing Radiation with Alzheimer's Disease Deaths in U.S. States. *J Alzheimers Dis*. 2017; 59:737–41.
<https://doi.org/10.3233/JAD-170308>
PMID:[28671130](https://pubmed.ncbi.nlm.nih.gov/28671130/)
 18. Iwata Y, Suzuki K, Wakuda T, Seki N, Thanseem I, Matsuzaki H, Mamiya T, Ueki T, Mikawa S, Sasaki T, Suda S, Yamamoto S, Tsuchiya KJ, et al. Irradiation in adulthood as a new model of schizophrenia. *PLoS One*. 2008; 3:e2283.
<https://doi.org/10.1371/journal.pone.0002283>
PMID:[18509473](https://pubmed.ncbi.nlm.nih.gov/18509473/)
 19. Loganovsky KN, Loganovskaja TK. Schizophrenia spectrum disorders in persons exposed to ionizing radiation as a result of the Chernobyl accident. *Schizophr Bull*. 2000; 26:751–73.
<https://doi.org/10.1093/oxfordjournals.schbul.a033492> PMID:[11087010](https://pubmed.ncbi.nlm.nih.gov/11087010/)
 20. Sibley RF, Moscato BS, Wilkinson GS, Natarajan N. Nested case-control study of external ionizing radiation dose and mortality from dementia within a pooled cohort of female nuclear weapons workers. *Am J Ind Med*. 2003; 44:351–58.
<https://doi.org/10.1002/ajim.10288>
PMID:[14502762](https://pubmed.ncbi.nlm.nih.gov/14502762/)
 21. Setkowicz Z, Gzielo-Jurek K, Uram Ł, Janicka D, Janeczko K. Brain dysplasia evoked by gamma irradiation at different stages of prenatal development leads to different tonic and clonic seizure reactivity. *Epilepsy Res*. 2014; 108:66–80.
<https://doi.org/10.1016/j.eplepsyres.2013.10.010>
PMID:[24239322](https://pubmed.ncbi.nlm.nih.gov/24239322/)
 22. Eriksson P. Developmental neurotoxicity of environmental agents in the neonate. *Neurotoxicology*. 1997; 18:719–26.
PMID:[9339819](https://pubmed.ncbi.nlm.nih.gov/9339819/)
 23. Semple BD, Blomgren K, Gimlin K, Ferriero DM, Noble-Haesslein LJ. Brain development in rodents and humans: Identifying benchmarks of maturation and vulnerability to injury across species. *Prog Neurobiol*. 2013; 106-107:1–16.
<https://doi.org/10.1016/j.pneurobio.2013.04.001>
PMID:[23583307](https://pubmed.ncbi.nlm.nih.gov/23583307/)
 24. Eriksson P, Buratovic S, Fredriksson A, Stenerlöv B, Sundell-Bergman S. Neonatal exposure to whole body ionizing radiation induces adult neurobehavioural defects: Critical period, dose–response effects and strain and sex comparison. *Behav Brain Res*. 2016; 304:11–19.
<https://doi.org/10.1016/j.bbr.2016.02.008>
PMID:[26876140](https://pubmed.ncbi.nlm.nih.gov/26876140/)
 25. Hennebert O, Laudenbach V, Laquerriere A, Verney C, Carmeliet P, Marret S, Leroux P. Ontogenic study of the influence of tissue plasminogen activator (t-PA) in neonatal excitotoxic brain insult and the subsequent microglia/macrophage activation. *Neuroscience*. 2005; 130:697–712.

- <https://doi.org/10.1016/j.neuroscience.2004.09.049>
PMID:15590153
26. McAuliffe JJ, Joseph B, Hughes E, Miles L, Vorhees CV. Metallothionein I,II deficient mice do not exhibit significantly worse long-term behavioral outcomes following neonatal hypoxia-ischemia: MT-I,II deficient mice have inherent behavioral impairments. *Brain Res*. 2008; 1190:175–85.
<https://doi.org/10.1016/j.brainres.2007.11.038>
PMID:18083145
27. Niatsetskeya ZV, Sosunov SA, Matsiukevich D, Utkina-Sosunova IV, Ratner VI, Starkov AA, Ten VS. The oxygen free radicals originating from mitochondrial complex I contribute to oxidative brain injury following hypoxia-ischemia in neonatal mice. *J Neurosci*. 2012; 32:3235–44.
<https://doi.org/10.1523/JNEUROSCI.6303-11.2012>
PMID:22378894
28. Al Mamun A, Yu H, Romana S, Liu F. Inflammatory Responses are Sex Specific in Chronic Hypoxic-Ischemic Encephalopathy. *Cell Transplant*. 2018; 27:1328–39.
<https://doi.org/10.1177/0963689718766362>
PMID:29692197
29. Brandt MD, Jessberger S, Steiner B, Kronenberg G, Reuter K, Bick-Sander A, von der Behrens W, Kempermann G. Transient calretinin expression defines early postmitotic step of neuronal differentiation in adult hippocampal neurogenesis of mice. *Mol Cell Neurosci*. 2003; 24:603–13.
[https://doi.org/10.1016/s1044-7431\(03\)00207-0](https://doi.org/10.1016/s1044-7431(03)00207-0)
PMID:14664811
30. Nowak E, Etienne O, Millet P, Lages CS, Mathieu C, Mouthon MA, Boussin FD. Radiation-induced H2AX phosphorylation and neural precursor apoptosis in the developing brain of mice. *Radiat Res*. 2006; 165:155–64.
<https://doi.org/10.1667/rr3496.1>
PMID:16435914
31. Olive PL, Banáth JP. Phosphorylation of histone H2AX as a measure of radiosensitivity. *Int J Radiat Oncol Biol Phys*. 2004; 58:331–35.
<https://doi.org/10.1016/j.ijrobp.2003.09.028>
PMID:14751500
32. Gajdusek C, Onoda K, London S, Johnson M, Morrison R, Mayberg M. Early molecular changes in irradiated aortic endothelium. *J Cell Physiol*. 2001; 188:8–23.
<https://doi.org/10.1002/jcp.1091> PMID:11382918
33. Valle I, Alvarez-Barrientos A, Arza E, Lamas S, Monsalve M. PGC-1alpha regulates the mitochondrial antioxidant defense system in vascular endothelial cells. *Cardiovasc Res*. 2005; 66:562–73.
<https://doi.org/10.1016/j.cardiores.2005.01.026>
PMID:15914121
34. Ungvari Z, Podlutzky A, Sosnowska D, Tucsek Z, Toth P, Deak F, Gautam T, Csiszar A, Sonntag WE. Ionizing radiation promotes the acquisition of a senescence-associated secretory phenotype and impairs angiogenic capacity in cerebrovascular endothelial cells: role of increased DNA damage and decreased DNA repair capacity in microvascular radiosensitivity. *J Gerontol A Biol Sci Med Sci*. 2013; 68:1443–57.
<https://doi.org/10.1093/gerona/glt057>
PMID:23689827
35. Hennicke T, Nieweg K, Brockmann N, Kassack MU, Gottmann K, Fritz G. mESC-based *in vitro* differentiation models to study vascular response and functionality following genotoxic insults. *Toxicol Sci*. 2015; 144:138–50.
<https://doi.org/10.1093/toxsci/kfu264>
PMID:25516496
36. Lafargue A, Degorre C, Corre I, Alves-Guerra MC, Gaugler MH, Vallette F, Pecqueur C, Paris F. Ionizing radiation induces long-term senescence in endothelial cells through mitochondrial respiratory complex II dysfunction and superoxide generation. *Free Radic Biol Med*. 2017; 108:750–59.
<https://doi.org/10.1016/j.freeradbiomed.2017.04.019>
PMID:28431961
37. Boström M, Kalm M, Eriksson Y, Bull C, Ståhlberg A, Björk-Eriksson T, Hellström Erkenstam N, Blomgren K. A role for endothelial cells in radiation-induced inflammation. *Int J Radiat Biol*. 2018; 94:259–71.
<https://doi.org/10.1080/09553002.2018.1431699>
PMID:29359989
38. Wang H, Segaran RC, Chan LY, Aladresi AA, Chinnathambi A, Alharbi SA, Sethi G, Tang FR. Gamma Radiation-Induced Disruption of Cellular Junctions in HUVECs Is Mediated through Affecting MAPK/NF- κ B Inflammatory Pathways. *Oxid Med Cell Longev*. 2019; 2019:1486232.
<https://doi.org/10.1155/2019/1486232>
PMID:31467629
39. Gaber MW, Yuan H, Killmar JT, Naimark MD, Kiani MF, Merchant TE. An intravital microscopy study of radiation-induced changes in permeability and leukocyte-endothelial cell interactions in the microvessels of the rat pia mater and cremaster muscle. *Brain Res Brain Res Protoc*. 2004; 13:1–10.
<https://doi.org/10.1016/j.brainresprot.2003.11.005>
PMID:15063835
40. Boström M, Hellström Erkenstam N, Kaluza D, Jakobsson L, Kalm M, Blomgren K. The hippocampal neurovascular niche during normal development and after irradiation to the juvenile mouse brain. *Int J Radiat Biol*. 2014; 90:778–89.

- <https://doi.org/10.3109/09553002.2014.931612>
PMID:[24913294](https://pubmed.ncbi.nlm.nih.gov/24913294/)
41. Boström M, Kalm M, Karlsson N, Hellström Erkenstam N, Blomgren K. Irradiation to the young mouse brain caused long-term, progressive depletion of neurogenesis but did not disrupt the neurovascular niche. *J Cereb Blood Flow Metab.* 2013; 33:935–43.
<https://doi.org/10.1038/jcbfm.2013.34>
PMID:[23486289](https://pubmed.ncbi.nlm.nih.gov/23486289/)
 42. Xiong S, Salazar G, Patrushev N, Ma M, Forouzandeh F, Hilenski L, Alexander RW. Peroxisome proliferator-activated receptor γ coactivator-1 α is a central negative regulator of vascular senescence. *Arterioscler Thromb Vasc Biol.* 2013; 33:988–98.
<https://doi.org/10.1161/ATVBAHA.112.301019>
PMID:[23430617](https://pubmed.ncbi.nlm.nih.gov/23430617/)
 43. Kim SB, Heo JI, Kim H, Kim KS. Acetylation of PGC1 α by Histone Deacetylase 1 Downregulation Is Implicated in Radiation-Induced Senescence of Brain Endothelial Cells. *J Gerontol A Biol Sci Med Sci.* 2019; 74:787–93.
<https://doi.org/10.1093/gerona/gly167>
PMID:[30016403](https://pubmed.ncbi.nlm.nih.gov/30016403/)
 44. Zhou K, Boström M, Ek CJ, Li T, Xie C, Xu Y, Sun Y, Blomgren K, Zhu C. Radiation induces progenitor cell death, microglia activation, and blood-brain barrier damage in the juvenile rat cerebellum. *Sci Rep.* 2017; 7:46181.
<https://doi.org/10.1038/srep46181> PMID:[28382975](https://pubmed.ncbi.nlm.nih.gov/28382975/)
 45. Roper SN, Eisenschenk S, King MA. Reduced density of parvalbumin- and calbindin D28-immunoreactive neurons in experimental cortical dysplasia. *Epilepsy Res.* 1999; 37:63–71.
[https://doi.org/10.1016/s0920-1211\(99\)00035-2](https://doi.org/10.1016/s0920-1211(99)00035-2)
PMID:[10515176](https://pubmed.ncbi.nlm.nih.gov/10515176/)
 46. Zhu WJ, Roper SN. Reduced inhibition in an animal model of cortical dysplasia. *J Neurosci.* 2000; 20: 8925–31.
<https://doi.org/10.1523/JNEUROSCI.20-23-08925.2000>
PMID:[11102503](https://pubmed.ncbi.nlm.nih.gov/11102503/)
 47. Schmidt SL, Vitral RW, Linden R. Effects of prenatal ionizing irradiation on the development of the ganglion cell layer of the mouse retina. *Int J Dev Neurosci.* 2001; 19:469–73.
[https://doi.org/10.1016/s0736-5748\(00\)00068-x](https://doi.org/10.1016/s0736-5748(00)00068-x)
PMID:[11378306](https://pubmed.ncbi.nlm.nih.gov/11378306/)
 48. Guo YR, Liu ZW, Peng S, Duan MY, Feng JW, Wang WF, Xu YH, Tang X, Zhang XZ, Ren BX, Tang FR. The Neuroprotective Effect of Amitriptyline on Radiation-Induced Impairment of Hippocampal Neurogenesis. *Dose Response.* 2019; 17:1559325819895912.
<https://doi.org/10.1177/1559325819895912>
PMID:[31903069](https://pubmed.ncbi.nlm.nih.gov/31903069/)
 49. Peng S, Yang B, Duan MY, Liu ZW, Wang WF, Zhang XZ, Ren BX, Tang FR. The Disparity of Impairment of Neurogenesis and Cognition After Acute or Fractionated Radiation Exposure in Adolescent BALB/c Mice. *Dose Response.* 2019; 17:1559325818822574.
<https://doi.org/10.1177/1559325818822574>.
PMID:[30670940](https://pubmed.ncbi.nlm.nih.gov/30670940/)
 50. Ueno H, Suemitsu S, Murakami S, Kitamura N, Wani K, Matsumoto Y, Okamoto M, Ishihara T. Region-specific reduction of parvalbumin neurons and behavioral changes in adult mice following single exposure to cranial irradiation. *Int J Radiat Biol.* 2019; 95:611–25.
<https://doi.org/10.1080/09553002.2019.1564081>
PMID:[30601685](https://pubmed.ncbi.nlm.nih.gov/30601685/)
 51. Wang SW, Ren BX, Qian F, Luo XZ, Tang X, Peng XC, Huang JR, Tang FR. Radioprotective effect of epimedium on neurogenesis and cognition after acute radiation exposure. *Neurosci Res.* 2019; 145:46–53.
<https://doi.org/10.1016/j.neures.2018.08.011>
PMID:[30145270](https://pubmed.ncbi.nlm.nih.gov/30145270/)
 52. Zanni G, Zhou K, Riebe I, Xie C, Zhu C, Hanse E, Blomgren K. Irradiation of the Juvenile Brain Provokes a Shift from Long-Term Potentiation to Long-Term Depression. *Dev Neurosci.* 2015; 37:263–72.
<https://doi.org/10.1159/000430435>
PMID:[26043717](https://pubmed.ncbi.nlm.nih.gov/26043717/)
 53. Reichelt AC, Killcross S, Hambly LD, Morris MJ, Westbrook RF. Impact of adolescent sucrose access on cognitive control, recognition memory, and parvalbumin immunoreactivity. *Learn Mem.* 2015; 22:215–24.
<https://doi.org/10.1101/lm.038000.114>
PMID:[25776039](https://pubmed.ncbi.nlm.nih.gov/25776039/)
 54. Soares AR, Gildawie KR, Honeycutt JA, Brenhouse HC. Region-specific effects of maternal separation on oxidative stress accumulation in parvalbumin neurons of male and female rats. *Behav Brain Res.* 2020; 388:112658.
<https://doi.org/10.1016/j.bbr.2020.112658>
PMID:[32339550](https://pubmed.ncbi.nlm.nih.gov/32339550/)
 55. Roughton K, Boström M, Kalm M, Blomgren K. Irradiation to the young mouse brain impaired white matter growth more in females than in males. *Cell Death Dis.* 2013; 4:e897.
<https://doi.org/10.1038/cddis.2013.423>
PMID:[24176855](https://pubmed.ncbi.nlm.nih.gov/24176855/)
 56. Boström M, Eriksson Y, Danial J, Björk-Eriksson T, Kalm M. Chronic disturbance in the thalamus following cranial irradiation to the developing mouse brain. *Sci Rep.* 2019; 9:9588.
<https://doi.org/10.1038/s41598-019-45973-8>
PMID:[31270437](https://pubmed.ncbi.nlm.nih.gov/31270437/)

57. Mukherjee B, Kessinger C, Kobayashi J, Chen BP, Chen DJ, Chatterjee A, Burma S. DNA-PK phosphorylates histone H2AX during apoptotic DNA fragmentation in mammalian cells. *DNA Repair (Amst)*. 2006; 5:575–90. <https://doi.org/10.1016/j.dnarep.2006.01.011> PMID:[16567133](https://pubmed.ncbi.nlm.nih.gov/16567133/)
58. Cordelli E, Eleuteri P, Grollino MG, Benassi B, Blandino G, Bartoleschi C, Pardini MC, Di Caprio EV, Spanò M, Pacchierotti F, Villani P. Direct and delayed X-ray-induced DNA damage in male mouse germ cells. *Environ Mol Mutagen*. 2012; 53:429–39. <https://doi.org/10.1002/em.21703> PMID:[22730201](https://pubmed.ncbi.nlm.nih.gov/22730201/)
59. Bekeschus S, Schütz CS, Nießner F, Wende K, Weltmann KD, Gelbrich N, von Woedtke T, Schmidt A, Stope MB. Elevated H2AX Phosphorylation Observed with kINPen Plasma Treatment Is Not Caused by ROS-Mediated DNA Damage but Is the Consequence of Apoptosis. *Oxid Med Cell Longev*. 2019; 2019:8535163. <https://doi.org/10.1155/2019/8535163> PMID:[31641425](https://pubmed.ncbi.nlm.nih.gov/31641425/)
60. Rogakou EP, Nieves-Neira W, Boon C, Pommier Y, Bonner WM. Initiation of DNA fragmentation during apoptosis induces phosphorylation of H2AX histone at serine 139. *J Biol Chem*. 2000; 275:9390–95. <https://doi.org/10.1074/jbc.275.13.9390> PMID:[10734083](https://pubmed.ncbi.nlm.nih.gov/10734083/)
61. Chang IY, Kim JH, Cho KW, Yoon SP. Acute responses of DNA repair proteins and StarD6 in rat hippocampus after domoic acid-induced excitotoxicity. *Acta Histochem*. 2013; 115:234–39. <https://doi.org/10.1016/j.acthis.2012.07.001> PMID:[22883302](https://pubmed.ncbi.nlm.nih.gov/22883302/)
62. Bigagli E, Luceri C, Scartabelli T, Dolara P, Casamenti F, Pellegrini-Giampietro DE, Giovannelli L. Long-term Neuroglial Cocultures as a Brain Aging Model: Hallmarks of Senescence, MicroRNA Expression Profiles, and Comparison With *In Vivo* Models. *J Gerontol A Biol Sci Med Sci*. 2016; 71:50–60. <https://doi.org/10.1093/gerona/glu231> PMID:[25568096](https://pubmed.ncbi.nlm.nih.gov/25568096/)
63. Yang Y, Wu N, Tian S, Li F, Hu H, Chen P, Cai X, Xu L, Zhang J, Chen Z, Ge J, Yu K, Zhuang J. Lithium promotes DNA stability and survival of ischemic retinal neurocytes by upregulating DNA ligase IV. *Cell Death Dis*. 2016; 7:e2473. <https://doi.org/10.1038/cddis.2016.341> PMID:[27853172](https://pubmed.ncbi.nlm.nih.gov/27853172/)
64. Romero AM, Palanca A, Ruiz-Soto M, Llorca J, Marín MP, Renau-Piqueras J, Berciano MT, Lafarga M. Chronic Alcohol Exposure Decreases 53BP1 Protein Levels Leading to a Defective DNA Repair in Cultured Primary Cortical Neurons. *Neurotox Res*. 2016; 29:69–79. <https://doi.org/10.1007/s12640-015-9554-8> PMID:[26264240](https://pubmed.ncbi.nlm.nih.gov/26264240/)
65. Suman S, Kumar S, N’Gouemo P, Datta K. Increased DNA double-strand break was associated with downregulation of repair and upregulation of apoptotic factors in rat hippocampus after alcohol exposure. *Alcohol*. 2016; 54:45–50. <https://doi.org/10.1016/j.alcohol.2016.06.003> PMID:[27565756](https://pubmed.ncbi.nlm.nih.gov/27565756/)
66. Hudson D, Kovalchuk I, Koturbash I, Kolb B, Martin OA, Kovalchuk O. Induction and persistence of radiation-induced DNA damage is more pronounced in young animals than in old animals. *Aging (Albany NY)*. 2011; 3:609–20. <https://doi.org/10.18632/aging.100340> PMID:[21685513](https://pubmed.ncbi.nlm.nih.gov/21685513/)
67. Cramer CK, Yoon SW, Reinsvold M, Joo KM, Norris H, Hood RC, Adamson JD, Klein RC, Kirsch DG, Oldham M. Treatment Planning and Delivery of Whole Brain Irradiation with Hippocampal Avoidance in Rats. *PLoS One*. 2015; 10:e0143208. <https://doi.org/10.1371/journal.pone.0143208> PMID:[26636762](https://pubmed.ncbi.nlm.nih.gov/26636762/)
68. Hamilton ME, Bols NC, Duncker BP. The characterization of γ H2AX and p53 as biomarkers of genotoxic stress in a rainbow trout (*Oncorhynchus mykiss*) brain cell line. *Chemosphere*. 2018; 201:850–58. <https://doi.org/10.1016/j.chemosphere.2018.03.015> PMID:[29554631](https://pubmed.ncbi.nlm.nih.gov/29554631/)
69. Rodier F, Coppé JP, Patil CK, Hoeijmakers WA, Muñoz DP, Raza SR, Freund A, Campeau E, Davalos AR, Campisi J. Persistent DNA damage signalling triggers senescence-associated inflammatory cytokine secretion. *Nat Cell Biol*. 2009; 11:973–79. <https://doi.org/10.1038/ncb1909> PMID:[19597488](https://pubmed.ncbi.nlm.nih.gov/19597488/)
70. Kanu N, Penicud K, Hristova M, Wong B, Irvine E, Plattner F, Raivich G, Behrens A. The ATM cofactor ATMIN protects against oxidative stress and accumulation of DNA damage in the aging brain. *J Biol Chem*. 2010; 285:38534–42. <https://doi.org/10.1074/jbc.M110.145896> PMID:[20889973](https://pubmed.ncbi.nlm.nih.gov/20889973/)
71. Kühne M, Riballo E, Rief N, Rothkamm K, Jeggo PA, Löbrich M. A double-strand break repair defect in ATM-deficient cells contributes to radiosensitivity. *Cancer Res*. 2004; 64:500–08. <https://doi.org/10.1158/0008-5472.can-03-2384> PMID:[14744762](https://pubmed.ncbi.nlm.nih.gov/14744762/)
72. Yamauchi M, Oka Y, Yamamoto M, Niimura K,

- Uchida M, Kodama S, Watanabe M, Sekine I, Yamashita S, Suzuki K. Growth of persistent foci of DNA damage checkpoint factors is essential for amplification of G1 checkpoint signaling. *DNA Repair (Amst)*. 2008; 7:405–17.
<https://doi.org/10.1016/j.dnarep.2007.11.011>
PMID:18248856
73. Suzuki M, Suzuki K, Kodama S, Watanabe M. Interstitial chromatin alteration causes persistent p53 activation involved in the radiation-induced senescence-like growth arrest. *Biochem Biophys Res Commun*. 2006; 340:145–50.
<https://doi.org/10.1016/j.bbrc.2005.11.167>
PMID:16360120
74. Suzuki M, Suzuki K, Kodama S, Watanabe M. Phosphorylated histone H2AX foci persist on rejoined mitotic chromosomes in normal human diploid cells exposed to ionizing radiation. *Radiat Res*. 2006; 165:269–76.
<https://doi.org/10.1667/rr3508.1> PMID:16494514
75. Suzuki M, Suzuki K, Kodama S, Yamashita S, Watanabe M. Persistent amplification of DNA damage signal involved in replicative senescence of normal human diploid fibroblasts. *Oxid Med Cell Longev*. 2012; 2012:310534.
<https://doi.org/10.1155/2012/310534>
PMID:23050037
76. Groesser T, Chang H, Fontenay G, Chen J, Costes SV, Helen Barcellos-Hoff M, Parvin B, Rydberg B. Persistence of γ -H2AX and 53BP1 foci in proliferating and non-proliferating human mammary epithelial cells after exposure to γ -rays or iron ions. *Int J Radiat Biol*. 2011; 87:696–710.
<https://doi.org/10.3109/09553002.2010.549535>
PMID:21271785
77. Kruhlak MJ, Celeste A, Dellaire G, Fernandez-Capetillo O, Müller WG, McNally JG, Bazett-Jones DP, Nussenzweig A. Changes in chromatin structure and mobility in living cells at sites of DNA double-strand breaks. *J Cell Biol*. 2006; 172:823–34.
<https://doi.org/10.1083/jcb.200510015>
PMID:16520385
78. Farg MA, Konopka A, Soo KY, Ito D, Atkin JD. The DNA damage response (DDR) is induced by the C9orf72 repeat expansion in amyotrophic lateral sclerosis. *Hum Mol Genet*. 2017; 26:2882–96.
<https://doi.org/10.1093/hmg/ddx170>
PMID:28481984
79. Tapias V, Hu X, Luk KC, Sanders LH, Lee VM, Greenamyre JT. Synthetic alpha-synuclein fibrils cause mitochondrial impairment and selective dopamine neurodegeneration in part via iNOS-mediated nitric oxide production. *Cell Mol Life Sci*. 2017; 74:2851–74.
<https://doi.org/10.1007/s00018-017-2541-x>
PMID:28534083
80. Yu H, Harrison FE, Xia F. Altered DNA repair; an early pathogenic pathway in Alzheimer’s disease and obesity. *Sci Rep*. 2018; 8:5600.
<https://doi.org/10.1038/s41598-018-23644-4>
PMID:29618789
81. Wang JY, Lai CL, Lee CT, Lin CY. Electronegative Low-Density Lipoprotein L5 Impairs Viability and NGF-Induced Neuronal Differentiation of PC12 Cells via LOX-1. *Int J Mol Sci*. 2017; 18:1744.
<https://doi.org/10.3390/ijms18081744>
PMID:28800073
82. Anderson DL, Mirzayans R, Andrais B, Siegbahn EA, Fallone BG, Warkentin B. Spatial and temporal distribution of γ H2AX fluorescence in human cell cultures following synchrotron-generated X-ray microbeams: lack of correlation between persistent γ H2AX foci and apoptosis. *J Synchrotron Radiat*. 2014; 21:801–10.
<https://doi.org/10.1107/S1600577514011424>
PMID:24971978
83. Silva AR, Santos AC, Farfel JM, Grinberg LT, Ferretti RE, Campos AH, Cunha IW, Begnami MD, Rocha RM, Carraro DM, de Bragança Pereira CA, Jacob-Filho W, Brentani H. Repair of oxidative DNA damage, cell-cycle regulation and neuronal death may influence the clinical manifestation of Alzheimer’s disease. *PLoS One*. 2014; 9:e99897.
<https://doi.org/10.1371/journal.pone.0099897>
PMID:24936870
84. Siddiqui MS, Francois M, Hecker J, Faunt J, Fenech MF, Leifert WR. γ H2AX is increased in peripheral blood lymphocytes of Alzheimer’s disease patients in the South Australian Neurodegeneration, Nutrition and DNA Damage (SAND) study of aging. *Mutat Res Genet Toxicol Environ Mutagen*. 2018; 829-830:6–18.
<https://doi.org/10.1016/j.mrgentox.2018.03.001>
PMID:29704994
85. Shanbhag NM, Evans MD, Mao W, Nana AL, Seeley WW, Adame A, Rissman RA, Masliah E, Mucke L. Early neuronal accumulation of DNA double strand breaks in Alzheimer’s disease. *Acta Neuropathol Commun*. 2019; 7:77.
<https://doi.org/10.1186/s40478-019-0723-5>
PMID:31101070
86. Necchi D, Pinto A, Tillhon M, Dutto I, Serafini MM, Lanni C, Govoni S, Racchi M, Prospero E. Defective DNA repair and increased chromatin binding of DNA repair factors in Down syndrome fibroblasts. *Mutat Res*. 2015; 780:15–23.
<https://doi.org/10.1016/j.mrfmmm.2015.07.009>
PMID:26258283

87. Huang C, Chu JM, Liu Y, Chang RC, Wong GT. Varenicline reduces DNA damage, tau mislocalization and post surgical cognitive impairment in aged mice. *Neuropharmacology*. 2018; 143:217–27.
<https://doi.org/10.1016/j.neuropharm.2018.09.044>
PMID:[30273594](https://pubmed.ncbi.nlm.nih.gov/30273594/)
88. Mata-Garrido J, Casafont I, Tapia O, Berciano MT, Lafarga M. Neuronal accumulation of unrepaired DNA in a novel specific chromatin domain: structural, molecular and transcriptional characterization. *Acta Neuropathol Commun*. 2016; 4:41.
<https://doi.org/10.1186/s40478-016-0312-9>
PMID:[27102221](https://pubmed.ncbi.nlm.nih.gov/27102221/)
89. Mata-Garrido J, Tapia O, Casafont I, Berciano MT, Cuadrado A, Lafarga M. Persistent accumulation of unrepaired DNA damage in rat cortical neurons: nuclear organization and ChIP-seq analysis of damaged DNA. *Acta Neuropathol Commun*. 2018; 6:68.
<https://doi.org/10.1186/s40478-018-0573-6>
PMID:[30049290](https://pubmed.ncbi.nlm.nih.gov/30049290/)
90. Yang ES, Newsheen S, Wang T, Thotala DK, Xia F. Glycogen synthase kinase 3beta inhibition enhances repair of DNA double-strand breaks in irradiated hippocampal neurons. *Neuro Oncol*. 2011; 13:459–70.
<https://doi.org/10.1093/neuonc/nor016>
PMID:[21398658](https://pubmed.ncbi.nlm.nih.gov/21398658/)
91. Nguyen P, Shukla S, Liu R, Abbineni G, Smart DK. Sirt2 Regulates Radiation-Induced Injury. *Radiat Res*. 2019; 191:398–412.
<https://doi.org/10.1667/RR15282.1>
PMID:[30835165](https://pubmed.ncbi.nlm.nih.gov/30835165/)
92. Ren BX, Huen I, Wu ZJ, Wang H, Duan MY, Guenther I, Bhanu Prakash KN, Tang FR. Early postnatal irradiation-induced age-dependent changes in adult mouse brain: MRI based characterization. *BMC Neurosci*. 2021; 22:28.
<https://doi.org/10.1186/s12868-021-00635-2>
PMID:[33882822](https://pubmed.ncbi.nlm.nih.gov/33882822/)